NCG-hIL2

Strain Name：NOD/ShiLtJGpt-*Prkdc*^{em26Cd52}*Il2rg*^{em26Cd22}*H11*$^{em1Cin(CAG-hIL2)}$/Gpt

Strain type：Knock-in

Strain number：T017543

Background：NOD/ShiLtJGpt

Description

Severe immune-deficient strain NCG is established by CRISPR/Cas9 technology. Prkdc (Protein kinase, DNA activated, catalytic polypeptide) and Il2rg (Common gamma chain receptor) genes are knocked out on NOD/ShiltJGpt background. The genetic background of NOD/ShiltJGpt makes this line have natural immunodeficiency, such as complement system and macrophage defects[1]. At the same time, the Sirpα on NOD/ShiltJGpt has high affinity with human CD47, making it more suitable for colonization of human grafts (e.g. tumors and human cells) than other strains[2]. Loss of Prkdc gene leads to the inability of VDJ recombination to occur, resulting in the inability of T cells and B cells to mature. Il2rg is a common subunit of various interleukin cytokine receptors, and the inactivation of Il2rg leads to the loss of six different cytokine signaling pathways[3], resulting in NK cell defects[4]. Therefore, NCG is the most thorough mouse model of the immune-deficient to date, and is very suitable for Cell derived xenograft (CDX), Patient derived xenograft (PDX), human peripheral blood mononuclear cells (PBMC) and human hematopoietic stem cell ($CD34^+$ HSC) transplantation for immune reconstruction.

IL-2 (interleukin-2) is a pleiotropic cytokine produced by $CD4^+$ T cells, $CD8^+$ T cells, B cells and dendritic cells. IL-2 plays a crucial role in activating immune system and the maintenance of immune homeostasis[5,6]. The major function of IL-2 is to promote proliferation of $CD4^+$ T and $CD8^+$T and NK cells, and IL-2 exerts immunosuppressive and immunostimulatory effects by activating regulatory T (Treg) versus cytotoxic effector cells[6]. NCG-hIL2 strain, knocked in the humanized IL2 gene on an NCG strain, can support the colonization and activity of human T cells and NK cells. The NCG-hIL2 mice verified by phenotypic analysis can be matched with other cytokines humanized mouse strains and will become an important model for the reconstruction of the human immune system.

Strain strategy

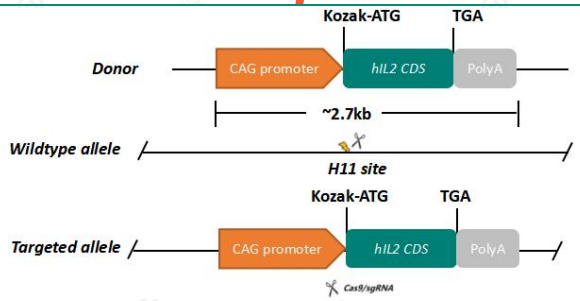

Fig 1. The diagram of humanized IL2 strategy in NCG-hIL2 mouse model.

Application

1. Humanized immune system reconstitution mouse model, eg. huPBMC and huPBNK and huCD34$^+$ HSC engraftment
2. Cell derived xenograft (CDX), Patient derived xenograft (PDX)
3. Immune-oncology therapy
4. Human hematopoietic and immune system research

Data support

1. hIL2 expression in various tissues detected at transcription level

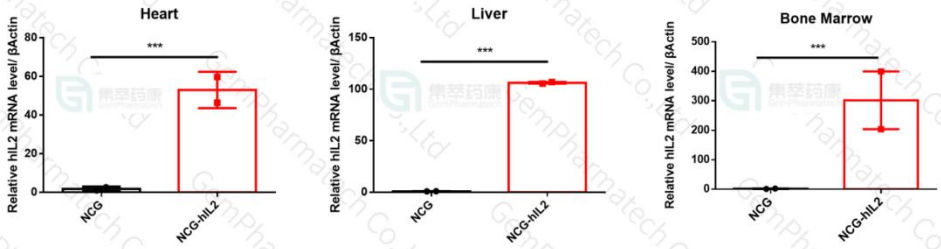

Fig 2. Comparison of human IL-2 expression in heart, liver and bone marrow from NCG and NCG-IL2 mice at transcription level.

Higher level of hIL2 was detected in heart, liver and bone narrow of NCG-hIL2 mice by q-PCR, while was not detected in those of NCG mice.

2. hIL2 protein expression analysis

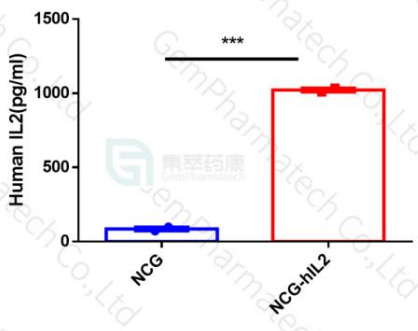

Fig 3. Comparison of human IL2 concentrations in plasma from NCG and NCG-IL2 mice.

Higher level of hIL2 was detected in the peripheral blood plasma of NCG-hIL2 mice by ELISA, while was not detected in that of NCG mice.

3. The diagram of huPBMC-NCG-hIL2 reconstitution

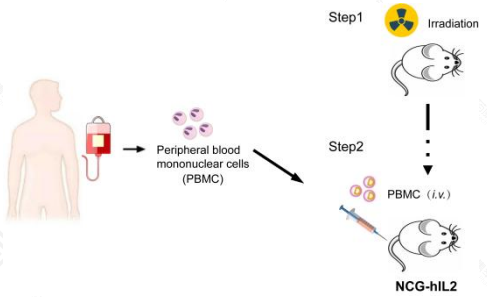

Fig 4. The diagram of huPBMC-NCG-hIL2 reconstitution process.

4. huPBMC-NCG-hIL2 mice prompted the human T cells reconstitution

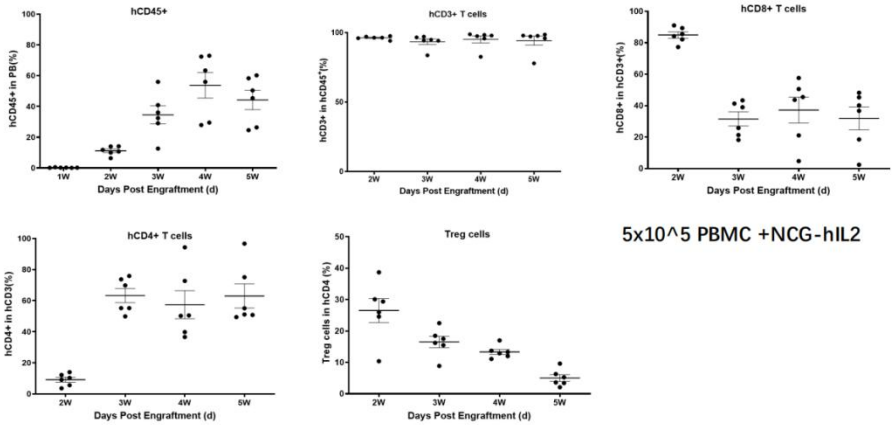

Fig 5. The reconstitution effects of huPBMC in NCG-hIL2 mice.

The immune cells reconstitution was high in huPBMC-NCG-hIL2 mice, mainly human $CD3^+$ T cells.

5. The life span of huPBMC-NCG-hIL2 mice

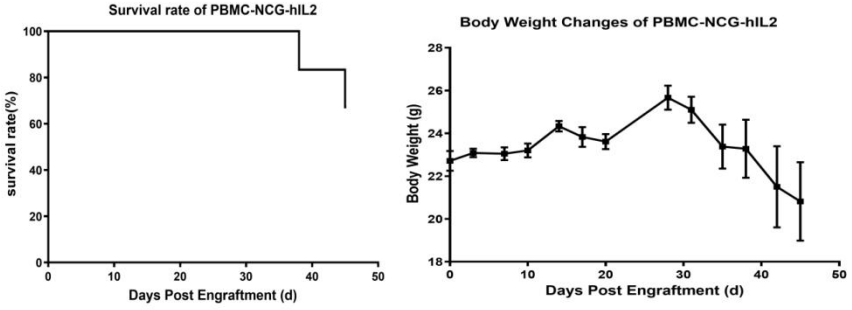

Fig 6. The survival rate and body weight change in huPBMC in NCG-hIL2 mice.

huPBMC-NCG-hIL2 mice had long survival and Nearly stable body weight changes.

6. The diagram of huHSC-NCG-hIL2 mice

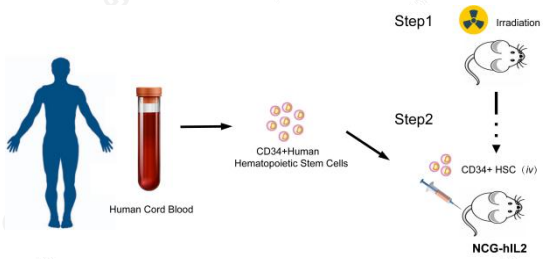

Fig 7. The diagram of huHSC-NCG-hIL2 reconstitution process.

7. The life span of huHSC-NCG-hIL2 mice

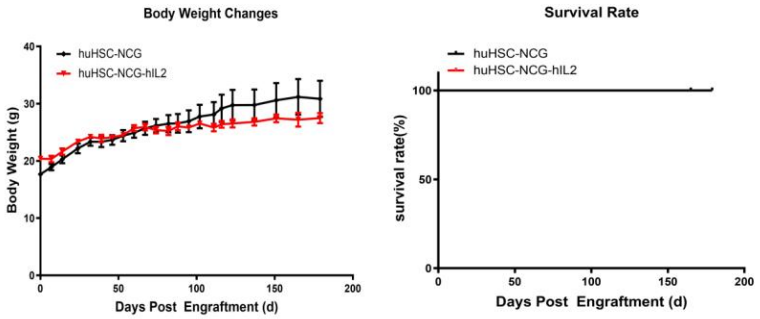

Fig 8. The survival rate and body weight change in huHSC in NCG-hIL2 mice.

huHSC-NCG-hIL2 mice had long survival and Nearly stable body weight changes.

8. huHSC-NCG-hIL2 mice prompted human NK cells reconstitution

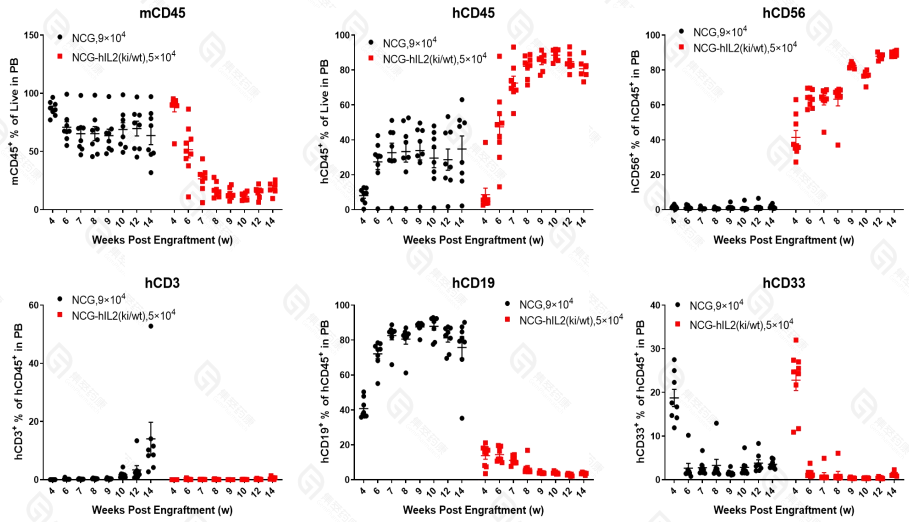

Fig 9. The reconstitution effect of huHSC in NCG-hIL2 mice.

Compared to huHSC-NCG, huHSC-NCG-hIL2 mice had a higher level of immune cells reconstitution with predominantly $hCD56^+$ NK cells and rarely $hCD3^+$ T, $hCD19^+$ B, and $hCD33^+$ myeloid cells.

9. CDX graft growth in huHSC-NCG-hIL2 mice

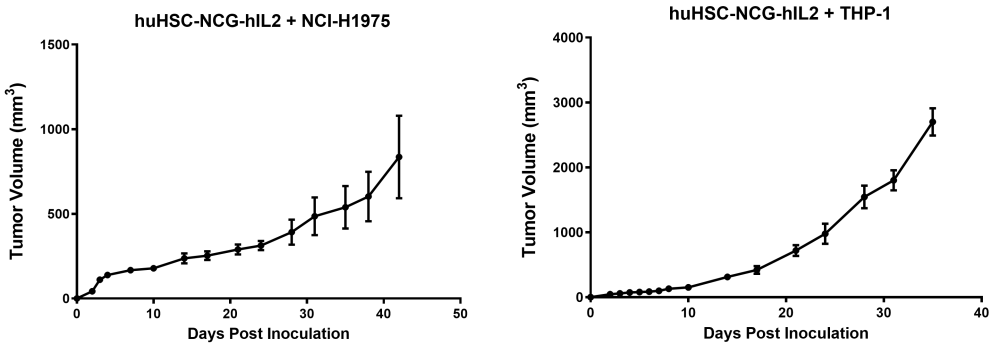

Fig 10. The reconstitution effect of huHSC in NCG-hIL2 mice.

NCI-H1975 and THP-1 tumor cell lines were inoculated subcutaneously into huHSC-NCG-hIL2 mice, respectively. It was found that both NCI-H1975 and THP-1 tumor cells could grow in huHSC-NCG-hIL2 mice.

10. Evaluation of ADCC effect of human NK cells from huHSC-NCG-hIL2 mice spleen in vitro

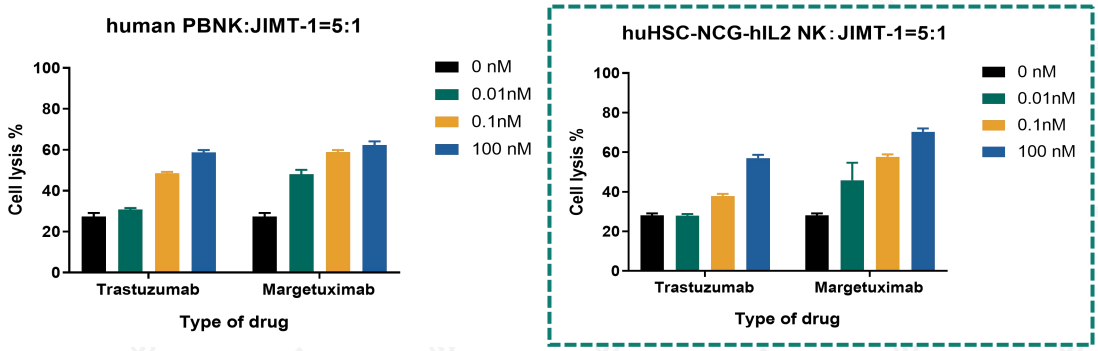

Fig 11. Evaluation of ADCC effect of NK cells from huHSC-NCG-hIL2 mice in vitro.

The human NK cells derived from the spleen of huHSC-NCG-hIL2 mice can effectively evaluate the dose-dependent effect of ADCC drugs in vitro, similar to human PBNK(Left figure). Additionally, it can also reflect the difference in ADCC effects between ADCC-regular (Trastuzumab) and ADCC-enhanced (Margetuximab) drugs(Right figure).

11. Evaluation of ADCC drugs in MDA-MB-453 subcutaneous transplanted tumor huHSC-NCG-hIL2 mice

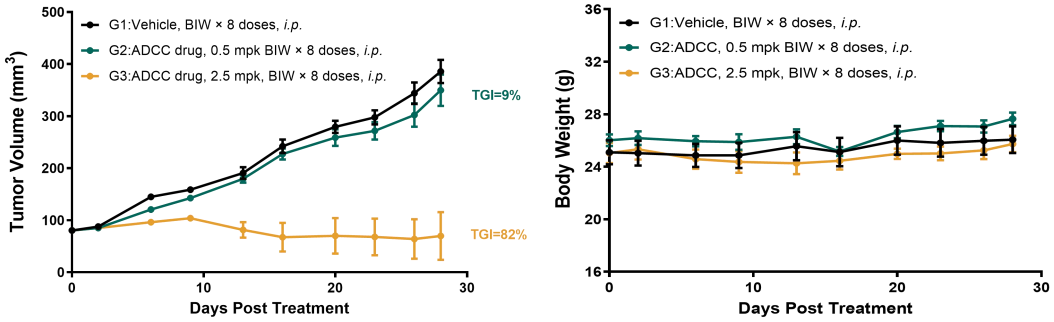

Fig 12. Efficacy of ADCC drugs in MDA-MB-453 transplanted huHSC-NCG-hIL2 mice.

The breast cancer MDA-MB-453 cells were inoculated subcutaneously into huHSC-NCG-hIL2 mice, and grouped when the tumor volume reached approximately 80 mm^3. Drug administration was performed on the day of grouping, and the dosage and schedule of drug administration were shown in the figure. The results revealed that the high dose of ADCC drug was able to inhibit the growth of MDA-MB-453 in vivo, suggesting that the drug was able to exert ADCC effect to kill the tumor cells through the reconstructed NK cells from HSC-NCG-hIL2 mice.

12. Evaluation of ADCC-enhanced drugs in JIMT-1 subcutaneous transplanted tumor huHSC-NCG-hIL2 mice

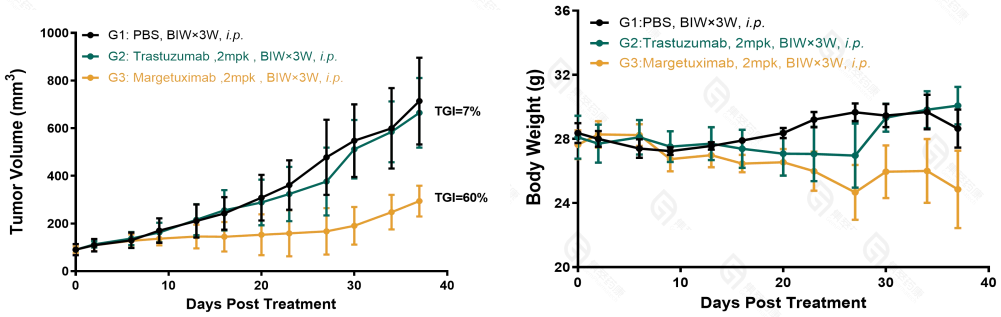

Fig 13. Efficacy of ADCC-enhanced drug in JIMT-1 transplanted huHSC-NCG-hIL2 mice.

The breast cancer JIMT-1 cells were inoculated subcutaneously into huHSC-NCG-hIL2 mice, and grouped when the tumor volume reached 80-120 mm^3. Dosing was performed on the day of grouping, and the schedule of administration was shown in the figure. The results revealed that compared with Trastuzumab (ADCC regular), the Margetuximab (ADCC enhanced) treatment group significantly inhibited tumor growth in huHSC-NCG-hIL2 mice in vivo.

13. The diagram of huPBNK-NCG-hIL2 mice

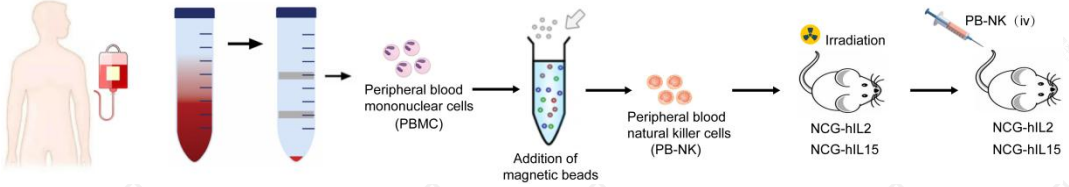

Fig 14. The diagram of huPBNK-NCG-hIL2 reconstitution process.

14. Immune reconstitution effects of huPBNK in NCG-hIL2 and NCG-hIL15 mice

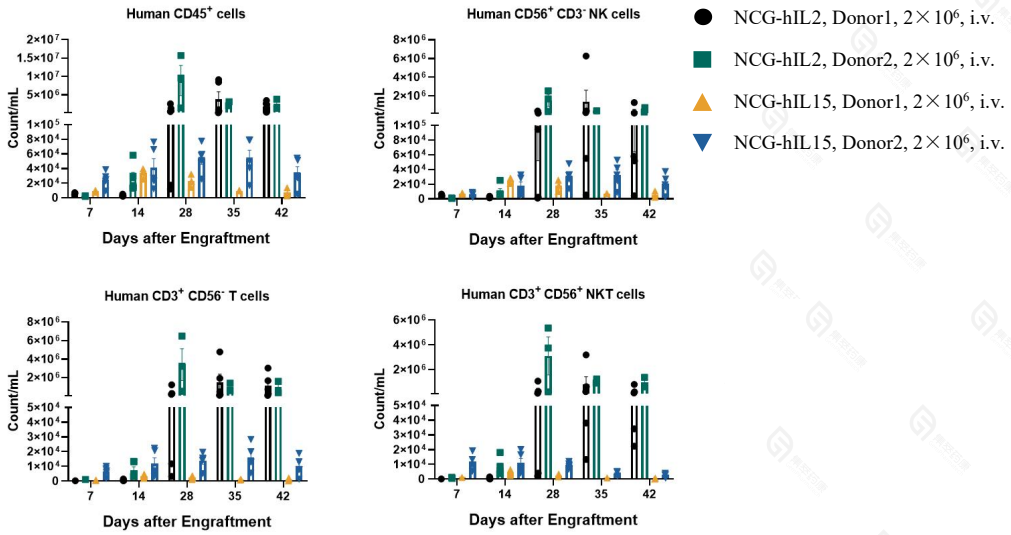

Fig 15. Immune reconstitution effects of huPBNK in NCG-hIL2 and NCG-hIL15 mice.

Peripheral blood of huPBNK-NCG-hIL2 and huPBNK-NCG-hIL15 mice was collected at 7, 14, 28, 35, and 42 days after huPBNK reconstitution for flow cytometry to detect hCD45, hCD3, and hCD56 markers expression. huPBNK- NCG-hIL15 mice were found to have higher levels of hCD45$^+$ immune cells, hCD56$^+$ hCD3$^-$ NK cells, hCD3$^+$ hCD56$^-$ T cells, and CD3$^+$ CD56$^+$ NK cells, as compared with huPBNK-NCG-hIL15 mice.

15. Reconstitution of huPBNK-NCG-hIL2 and huPBNK-NCG-hIL15 functional NK cells

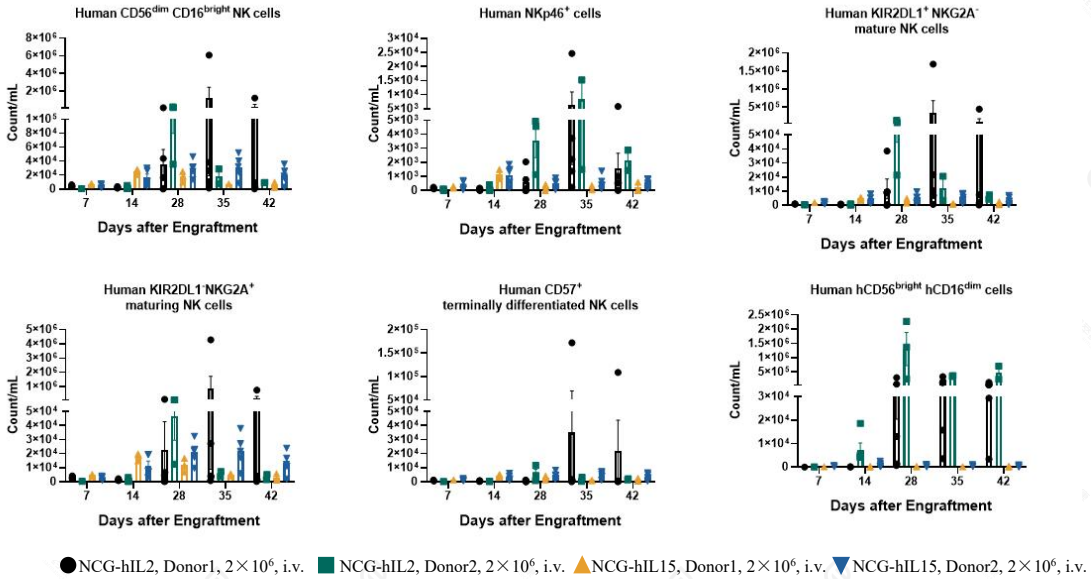

Fig 16. huPBNK-NCG-hIL2 and huPBNK-NCG-hIL15 reconstructed functional NK cells.

Peripheral blood of huPBNK-NCG-hIL2 and huPBNK-NCG-hIL15 mice was collected at 7, 14, 28, 35, and 42 days after huPBNK reconstitution, respectively, and flow cytometry was performed to detect functional NK cell-associated markers, hCD56, hCD16, hNKp46, hKIR2DL1, hNKG2A, and hCD57. The results revealed that huPBNK-NCG-hIL2 mice reconstituted higher levels of functional NK cells compared to huPBNK-NCG-hIL15 mice.

16. huPBNK-NCG-hIL2 mice promoted cytokine release

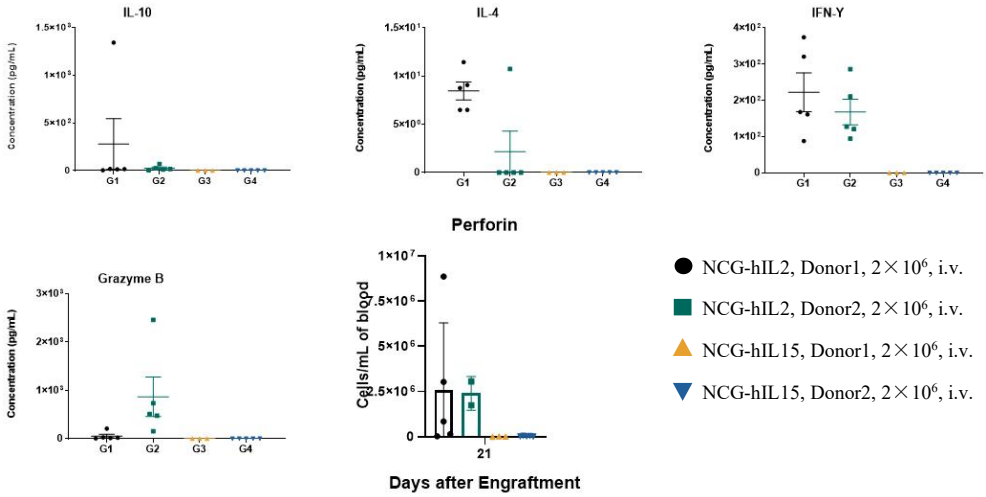

Fig 17. Cytokine release levels in huPBNK-NCG-hIL2 mice.

Peripheral blood from huPBNK-NCG-hIL2 and huPBNK-NCG-hIL15 mice was collected at 21 days after huPBNK reconstitution for CBA and flow cytometry to detect the concentration of IL-10, IL-4, IFN-Y, Grazyme B, and Perforin, respectively. huPBNK-NCG-hIL15 mice were found to release higher levels of L-10, IL-4, IFN-Y, Grazyme B, and Perforin, compared with huPBNK-NCG-hIL15 mice.

References

1.Shultz LD, Schweitzer PA, Christianson SW, et al. (1995). "Multiple defects in innate and adaptive immunologic function in NOD/LtSz-scid mice". J. Immunol. 154 (1): 180–91.

2.Takenaka K, Prasolava TK, Wang JC, et al. (2007). "Polymorphism in Sirpa modulates engraftment of human hematopoietic stem cells". Nat. Immunol. 8 (12): 1313–23.

3.Greiner DL, Hesselton RA, Shultz LD (1998). "SCID mouse models of human stem cell engraftment". Stem Cells. 16 (3): 166–177.

4.Cao X, Shores EW, Hu-Li J, et al. (1995). "Defective lymphoid development in mice lacking expression of the common cytokine receptor gamma chain". Immunity. 2 (3): 223–38.

5.Sarah L. Gaffena, Kathleen D. Liu. "Overview of interleukin-2 function, production and clinical applications"Cytokine 28 (2004) 109-123.
6.Natalia Arenas-Ramirez, Janine Woytschak, and Onur Boyman. " Interleukin-2: Biology, Design and Application" Trends in Immunology 12 (2015), 763-777.